

STRUCTURAL AND THEORETICAL STUDY OF SIX DINUCLEAR Co(II), Ni(II), Cu(II), Zn(II), Cd(II) and Hg(II) COMPLEXES CONTAINING ON-NO DONOR AZODYE LIGAND, 4,4'-(1E,1'E)-(5,5'-(PROPANE-2,2-DIYL)BIS(2-HYDROXY-5,1-PHENYLENE)BIS(DIAZENE-2,1-DIYL)DIBENZENESULFONIC ACID

Bipin Bihari Mahapatra^{1*}, Ashish Kumar Sarangi² and Ramani Ranjan Mishra¹

¹P.G. Department of Chemistry, G.M. College, Sambalpur, Odisha, India

²Department of Chemistry, Government College of Engineering Kalahandi, Bhawanipatna, Odisha, India

(Received February 28, 2015; revised December 26, 2015)

ABSTRACT. Six dimeric transitional metal complexes with ON-NO donor bis-bidentate azodye ligand 4,4'-(1E,1'E)-(5,5'-(propane-2,2-diyl)bis(2-hydroxy-5,1-phenylene)bis(diazene-2,1-diyl)dibenzenesulfonic acid (PDHPDDDBSA) have been synthesised and characterized by elemental, analytical, conductivity measurement, magnetic moments, spectral, thermal, X-ray diffraction (powder pattern) and theoretical methods. The Co(II) and Ni(II) complexes are found to be octahedral, Cu(II) complex is distorted-octahedral and a tetrahedral stereochemistry has been suggested to Zn(II), Cd(II) and Hg(II) complexes. The thermal analysis data provided the kinetic parameters as order of decomposition reaction, activation energy and frequency factor. All theoretical calculations of the ligand and the Cu(II) and Zn(II) complexes were made using Gaussian 03 rev. A.01 programme package hybrid DFT/B3LYP hybrid functional level of theory with LANL2DZ basic set for copper and zinc atoms in gas phase and 6-31 G(d,p) basic set for other atoms. The DFT study of the ligand and the complexes is used to calculate the bond length, bond angle, HOMO, LUMO and dipole moment values. The calculated HOMO-LUMO energy gap shows that a charge transfer occurs within the molecule. The Cd(II) complex is found to have an orthorhombic crystal system.

KEY WORDS: Azodye complexes, Thermogravimetric study, Theoretical study (DFT/B3LYP)

INTRODUCTION

A large number of publications have been made in recent years with azodye ligands containing nitrogen, oxygen and sulfur donor atoms and their metal complexes ranging from pure synthetic works to physicochemical and biological studies [1]. The azodyes have many applications in various fields as pharmaceutical industry as chemotherapeutics [2], chemical laboratory as indicators, chemical reactions as catalysts, textile industry as dyeing agents and food industry as preservatives [3]. Bisphenol A [2,2'-di(4-hydroxyphenyl) propane] is used to make plastic based commercial materials [4], colour developer in carbonless copy paper and thermal paper receipts [5, 6]. Sulphanilic acid is used to make sulphur drugs and dyes [7]. Keeping these wide applications in view, these two compounds are coupled to form a novel new ON-NO donor tetradentate azodye. In continuation to our previous works [8], we report here the synthesis of one bis-bidentate (tetradentate) azodye (Figure 1) and its six dimeric metal complexes. The characterization of these metal complexes was made by spectral, thermal, X-ray and theoretical studies.

EXPERIMENTAL

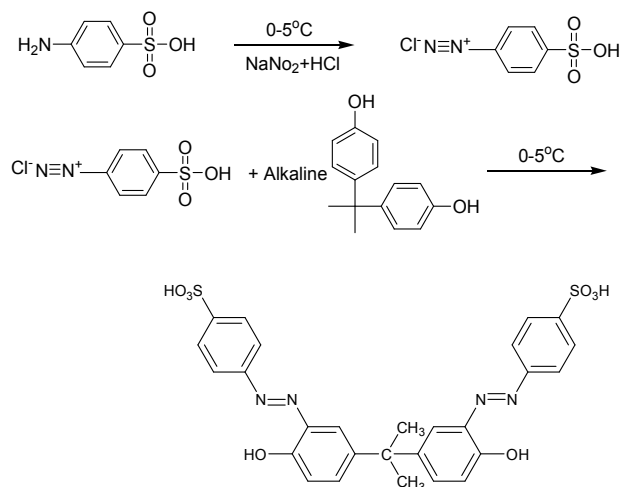
Materials

Sulphanilic acid and 2,2'-di(4-hydroxyphenyl) propane were E. Merck grade. The chlorides of Co(II), Ni(II), Cu(II), Zn(II), Cd(II) and Hg(II) were of S.R.L. grade. All other reagents and solvents were purchased from commercial sources and were of analytical grade.

*Corresponding author. E-mail: mahapatra.bipin@yahoo.com, 2 ashishsbp_2008@yahoo.com

Synthesis of the azodye ligand

Sulphanilic acid (0.02 mol, 3.46 g) on treatment with NaNO_2 and HCl form corresponding diazonium chloride that was then treated with an alkaline solution of 2,2'-di(4-hydroxyphenyl)propane (0.01 mol, 2.28 g) at 0-5 °C, when the azodye 4,4'-(1E,1'E)-(5,5'-(propane-2,2-diyl)bis(2-hydroxy-5,1-phenylene)bis(diazene-2,1-diyl)dibenzenesulfonic acid (PDHPDDDBSA) was obtained. $\text{LH}_2 = \text{C}_{27}\text{H}_{24}\text{N}_4\text{S}_2\text{O}_8$ (596.6), m.p. 115 °C. Anal. calc. (%) C, 54.36; H, 4.05; N, 9.39; S, 10.75; found (%) C, 54.1; H, 3.7; N, 9.2; S, 10.5. IR (KBr pellet cm^{-1}): 1509 $\nu(\text{C-O})$; 1597.9 $\nu(\text{N=N})$.



Scheme 1. 4,4'-(1E,1'E)-(5,5'-(propane-2,2-diyl)bis(2-hydroxy-5,1-phenylene)bis(diazene-2,1-diyl)dibenzenesulfonic acid (PDHPDDDBSA).

Synthesis of the metal complexes

The ethanolic solution of metal chlorides was mixed with ethanolic solution of the ligand in 2:1 molar ratio. The resulting solutions were heated to 50-60 °C for about one hour on a heating mantle and the pH was raised to ~7 by adding conc. NH_4OH drop by drop with stirring. The solid metal complexes thus formed were then washed with ethanol followed by ether and dried in vacuum.

$[\text{Co}_2(\text{PDHPDDDBSA})\text{Cl}_2(\text{H}_2\text{O})_6]$. (Dark brown) $\text{C}_{27}\text{H}_{34}\text{Cl}_2\text{Co}_2\text{N}_4\text{O}_{14}\text{S}_2$ (891.48), m.p. > 250 °C, anal. calc. (%) C, 36.38; H, 3.84; N, 6.28; S, 7.19; Cl, 7.95; Co, 13.22; found (%) C, 36.2; H, 3.5; N, 5.9; S, 6.8; Cl, 7.6; Co, 12.9, IR (KBr pellet cm^{-1}): 1485 $\nu(\text{C-O})$; 1562 $\nu(\text{N=N})$; 533.5 $\nu(\text{M-O})$; 456.9 $\nu(\text{M-N})$.

$[\text{Ni}_2(\text{PDHPDDDBSA})\text{Cl}_2(\text{H}_2\text{O})_6]$. (Dark green) $\text{C}_{27}\text{H}_{34}\text{Cl}_2\text{Ni}_2\text{N}_4\text{O}_{14}\text{S}_2$ (890.99), m.p. > 250 °C, anal. calc. (%) C, 36.4; H, 3.85; N, 6.29; S, 7.2; Cl, 7.96; Ni, 13.17; found (%) C, 36.1; H, 3.4; N, 5.8; S, 6.9; Cl, 7.5; Ni, 12.8, IR (KBr pellet cm^{-1}): 1480 $\nu(\text{C-O})$; 1560 $\nu(\text{N=N})$; 530 $\nu(\text{M-O})$; 450 $\nu(\text{M-N})$.

$[\text{Cu}_2(\text{PDHPDDDBSA})\text{Cl}_2(\text{H}_2\text{O})_6]$. (Grey) $\text{C}_{27}\text{H}_{34}\text{Cl}_2\text{Cu}_2\text{N}_4\text{O}_{14}\text{S}_2$ (900.70), m.p. > 250 °C, anal. calc. (%) C, 36.01; H, 3.8; N, 6.22; S, 7.12; Cl, 7.87; Cu, 14.11; found (%) C, 35.7; H, 3.5; N, 5.9; S, 6.7; Cl, 7.7; Cu, 13.9, IR (KBr pellet cm^{-1}): 1490 $\nu(\text{C-O})$; 1565 $\nu(\text{N=N})$; 530 $\nu(\text{M-O})$; 455 $\nu(\text{M-N})$.

$[Zn_2(PDHPDDDBSA)Cl_2(H_2O)_2]$. (Yellow) $C_{27}H_{26}Cl_2Zn_2N_4O_{10}S_2$ (832.33), m.p. > 250 °C, anal. calc. (%) C, 38.96; H, 3.15; N, 6.73; S, 7.7; Cl, 8.52; Zn, 15.71; found (%) C, 39.0; H, 3.4; N, 6.8; S, 7.9; Cl, 8.8; Zn, 15.9, IR (KBr pellet cm^{-1}): 1485 ν (C-O); 1560 ν (N=N); 525 ν (M-O); 450 ν (M-N).

$[Cd_2(PDHPDDDBSA)Cl_2(H_2O)_2]$. (Grey) $C_{27}H_{26}Cl_2Cd_2N_4O_{10}S_2$ (926.37), m.p. > 250 °C, anal. calc. (%) C, 35.01; H, 2.83; N, 6.05; S, 6.92; Cl, 7.65; Cd, 24.27; found (%) C, 35.3; H, 2.9; N, 6.3; S, 7.1; Cl, 7.9; Cd, 24.5, IR (KBr pellet cm^{-1}): 1480 ν (C-O); 1565 ν (N=N); 530 ν (M-O); 450 ν (M-N).

$[Hg_2(PDHPDDDBSA)Cl_2(H_2O)_2]$. (Yellow) $C_{27}H_{26}Cl_2Hg_2N_4O_{10}S_2$ (1102.75), m.p. > 250 °C, anal. calc. (%) C, 29.41; H, 2.38; N, 5.08; S, 5.81; Cl, 6.43; Hg, 36.38; found (%) C, 29.8; H, 2.5; N, 5.4; S, 5.9; Cl, 6.8; Hg, 36.6, IR (KBr pellet cm^{-1}): 1485 ν (C-O); 1560 ν (N=N); 525 ν (M-O); 455 ν (M-N).

Physical measurements

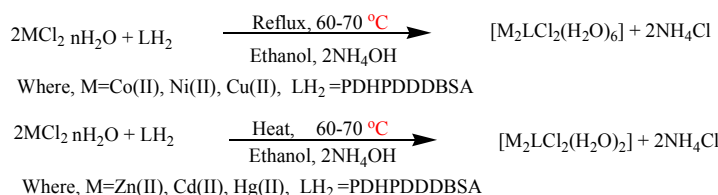
Elemental analysis (C, H, N and Cl) were carried out on elemental analyser Perkin-Elmer 2400 while metals were determined by EDTA after decomposing the complexes with conc. HNO_3 . Conductance measurements of the complexes were made using Toshniwal CL 01-06 Conductivity Bridge. The magnetic susceptibility were made at RT by Gouy method using $Hg[Co(CN)_4]$ as calibrant. IR Spectra (KBr pellet) were recorded using IFS 66U spectrophotometer, electronic spectra of the Co^{II} , Ni^{II} and Cu^{II} complexes in DMF were recorded on a Hilger-Watt uvispeck spectrophotometer, ESR spectra of Cu^{II} complex was recorded on a E_4 - spectrometer and NMR spectra on a Jeol GSX 400 with d_6 -DMSO as solvent and TMS as internal standard. X-Ray diffraction (powder pattern) of the Ni^{II} complex was recorded on a Phillips PW 1130/00 diffractometer with scan axis-Gonio, start position (2 θ -10.004) end position (2 θ -89.976) anode material CuK – ALPHA 1[\AA] = 1.54060 and the generator settings 30 mA, 40 kV. The TG, DTG and DTA of the complex were recorded on NETZSCH STA 409 C/CD in nitrogen atmosphere at a heating rate of 10 °C/min.

Theoretical (DFT/B3LYP) studies

The input file of ligand and the metal complexes $[Cu_2LCl_2(H_2O)_6]$, $[Zn_2LCl_2(H_2O)_2]$ were prepared with Gauss View 5.0.8 [9]. All theoretical calculations of the ligand and the complexes were made using GAUSSIAN 03 rev. A.01 programme package [10-16] hybrid DFT/B3LYP hybrid functional level of theory with LANL2DZ basic set for copper and zinc atoms in gas phase and 6-31 G(d, p) basic set for other atoms. The 6-31 G (d, p) is the almost popular and appropriate basic set that explains p function to all hydrogen atoms in addition to that d function for other heavy atoms and LANL2DZ basic set is suitable to all first row transition metal because it uses the calculation of effective core potential surfaces.

RESULTS AND DISCUSSION

The metal complexes were prepared according to the following reaction scheme:



The elemental analysis data agree well with the following composition of the metal complexes (Table 1), $[M_2LCl_2(H_2O)_6]$ and $[M'_2LCl_2(H_2O)_2]$ where $M = Co^{II}, Ni^{II}, Cu^{II}$; $M' = Zn^{II}, Cd^{II}, Hg^{II}$. All the complexes are semi-crystalline in nature and have high melting points. The complexes are insoluble in common organic solvents as methanol, ethanol and benzene but soluble in dimethylformamide and dimethyl sulphoxide. The complexes are non-electrolytic nature as evident from their low conductance values ($3.4\text{--}4.9 \Omega^{-1} \text{cm}^2 \text{mol}^{-1}$) in 10^{-3} M DMF solution.

IR spectra

In the IR spectrum of the ligand, one broad band is observed at 3344 cm^{-1} that can be attributed to intramolecular O-H...N hydrogen bonding. The absence of this band in the spectra of the metal complexes indicates deprotonation of the phenolic -OH groups and bonding of phenolic oxygen atom to the metal ion [17]. This is further supported by the shift of the band at 1509 cm^{-1} (LH_2) to $\sim 1485 \text{ cm}^{-1}$ in the metal complexes. The sharp band of the ligand at 1597.9 cm^{-1} can be attributed to $\nu_{(N=N)}$ vibration and in the metal complexes these bands shown at $\sim 1562 \text{ cm}^{-1}$, that indicates the coordination of one of the azo nitrogen atoms to the metal ions [18]. In the metal complexes broad band appears $\sim 3369 \text{ cm}^{-1}$ followed by sharp peaks at $\sim 829.5 \text{ cm}^{-1}$ and at $\sim 681.4 \text{ cm}^{-1}$ assignable to -OH stretching, rocking and wagging vibrations, respectively, indicating the presence of co-ordinated water molecules in the complexes [19]. The conclusive evidence of bonding of the ligand to the metal ions is proved by the appearance of bands at $\sim 533 \text{ cm}^{-1}$ (M-O) and $\sim 456 \text{ cm}^{-1}$ (M-N) [20].

Electronic spectra and magnetic measurements

In the electronic spectrum of Co^{II} complex, four ligand field bands appear at 8255, 16520, 20442 and 32390 cm^{-1} . The first three bands can be attributed to ${}^4T_{1g}(F) \rightarrow {}^4T_{2g}(F) (\nu_1)$, $\rightarrow {}^4A_{2g}(F) (\nu_2)$ and $\rightarrow {}^4T_{1g}(P) (\nu_3)$ transitions, respectively and the fourth band is assigned to a CT band [22]. It is well knowing that [21]

$$\begin{aligned} {}^4T_{1g}(F) &\rightarrow {}^4T_{2g}(F) (\nu_1), E \approx 8Dq \\ {}^4T_{1g}(F) &\rightarrow {}^4A_{2g}(F) (\nu_2), E \approx 18Dq \\ {}^4T_{1g}(F) &\rightarrow {}^4T_{1g}(P) (\nu_3), E \approx 6Dq + 15B \end{aligned}$$

From the above equations the following relations have been derived and the ligand field parameters as $Dq = 826.5 \text{ cm}^{-1}$, $B = 813.1 \text{ cm}^{-1}$, $\beta_{35} = 0.837 \text{ cm}^{-1}$, $\nu_2/\nu_1 = 2.001$ and $\sigma = 19.4\%$ have been calculated

$$\begin{aligned} Dq &= (\nu_2 - \nu_1)/10 \\ B &= (\nu_2 + \nu_3 - 3\nu_1)/15 \\ \beta_{35} &= B/971 \\ \sigma &= [(1 - \beta_{35})/\beta_{35}] \times 100 \end{aligned}$$

This suggests an octahedral geometry for the complex [23, 24]. In the electronic spectrum of Ni^{II} complex, four ligand field bands are observed at 10235, 17388, 24995 and 32750 cm^{-1} assignable to ${}^3A_{2g}(F) \rightarrow {}^3T_{2g}(F) (\nu_1)$, $\rightarrow {}^3T_{1g}(F) (\nu_2)$, $\rightarrow {}^3T_{1g}(P) (\nu_3)$ and CT transition [22], respectively in an octahedral geometry. It is also known that [21]

$$\begin{aligned} {}^3A_{2g}(F) &\rightarrow {}^3T_{2g}(F) (\nu_1), E \approx 10Dq \\ {}^3A_{2g}(F) &\rightarrow {}^3T_{1g}(F) (\nu_2), E \approx 18Dq \\ {}^3A_{2g}(F) &\rightarrow {}^3T_{1g}(P) (\nu_3), E \approx 12Dq + 15B \end{aligned}$$

From the above equations the following relations have been derived and the ligand field parameters as $Dq = 1023.5 \text{ cm}^{-1}$, $B = 778.5 \text{ cm}^{-1}$, $\beta_{35} = 0.778 \text{ cm}^{-1}$, $v_2/v_1 = 1.699$ and $\sigma = 33.83 \%$ have been calculated.

$$Dq = v_1/10$$

$$B = (v_2 + v_3 - 3v_1)/15$$

$$\beta_{35} = B/1041$$

$$\sigma = [(1-\beta_{35})/\beta_{35}] \times 100$$

This confirms an octahedral symmetry for the complex. The electronic spectrum of the copper(II) complex exhibit one broad band at $\sim 13360\text{-}14490 \text{ cm}^{-1}$ with maxima at $\sim 14370 \text{ cm}^{-1}$ assignable to ${}^2E_g \rightarrow {}^2T_{2g}$ transition in support of a distorted-octahedral configuration of the complex [25, 26]. The magnetic moment of high-spin of Co^{II} complexes are found in the range 4.7-5.2 B.M. [27, 28]. The observed magnetic moment of the Co^{II} complex is found to be 5.1 B.M. indicating octahedral configuration of the complex that is further supported by the electronic spectral data [29]. The magnetic moment values of Ni^{II} and Cu^{II} complexes are found to be 3.2 and 1.8 B.M. respectively indicating octahedral environment around the metal ions [30] (Table 1). These three complexes are no doubt binuclear in nature, they exhibit normal magnetic moments of mononuclear complexes attributable to absence of M-M interaction between the metal ions.

Table 1. Electronic spectra and magnetic moment data.

Complex	ν in (cm^{-1})	Transition	μ_{eff} in BM	Dq in (cm^{-1})	B in (cm^{-1})	β_{35} in (cm^{-1})	v_2/v_1	σ in %
[Co ₂ LCl ₂ (H ₂ O) ₆]	8255	${}^4T_{1g}(\text{F}) \rightarrow {}^4T_{2g}(\text{F})$ (ν_1)	5.1	826.5	813.1	0.837	2.001	19.47
	16520	${}^4T_{1g}(\text{F}) \rightarrow A_{2g}(\text{F})$ (ν_2)						
	20442	${}^4T_{1g}(\text{F}) \rightarrow {}^4T_{1g}(\text{P})$ (ν_3)						
	32390	CT band						
[Ni ₂ LCl ₂ (H ₂ O) ₆]	10235	${}^3A_{2g}(\text{F}) \rightarrow {}^3T_{2g}(\text{F})$ (ν_1)	3.2	1023.5	778.5	0.778	1.699	33.83
	17388	${}^3A_{2g}(\text{F}) \rightarrow {}^3T_{1g}(\text{F})$ (ν_2)						
	24995	${}^3A_{2g}(\text{F}) \rightarrow {}^3T_{1g}(\text{P})$ (ν_3)						
	32750	CT band						
[Cu ₂ LCl ₂ (H ₂ O) ₆]	13360-14490	${}^2E_g \rightarrow {}^2T_{2g}$	1.8	-	-	-	-	-

¹H-NMR studies

The ¹H NMR spectrum of the ligand LH₂ was recorded in DMSO_d₆. The complex pattern observed at δ 6.7310-7.2598 ppm corresponds to fourteen phenyl protons [31]. The sharp peak obtained at δ 1.6183 ppm corresponds to six methyl protons. The peak for phenolic proton (OH) was not observed as it is beyond the range of the instrument used (Figure 1).

ESR studies

The ESR spectrum of the copper(II) complex has been recorded at X-band at RT. The ' g_{av} ' value of the complex is found to be 2.036 by applying Kneubuhl's method [32]. This kind of spectrum

may be attributable to dynamic or pseudo rotational type of Jahn-Teller distortion. The spin-orbit coupling constant (λ) can be calculated from the relation [33]:

$$g_{av} = 2(1 - 2\lambda/10Dq)$$

The λ value of the complex is found to be -372.18 cm^{-1} . The decrease of the λ values from the free ion value (-830 cm^{-1}) indicates the overlapping of metal ligand orbitals in the metal complexes (Figure 2).

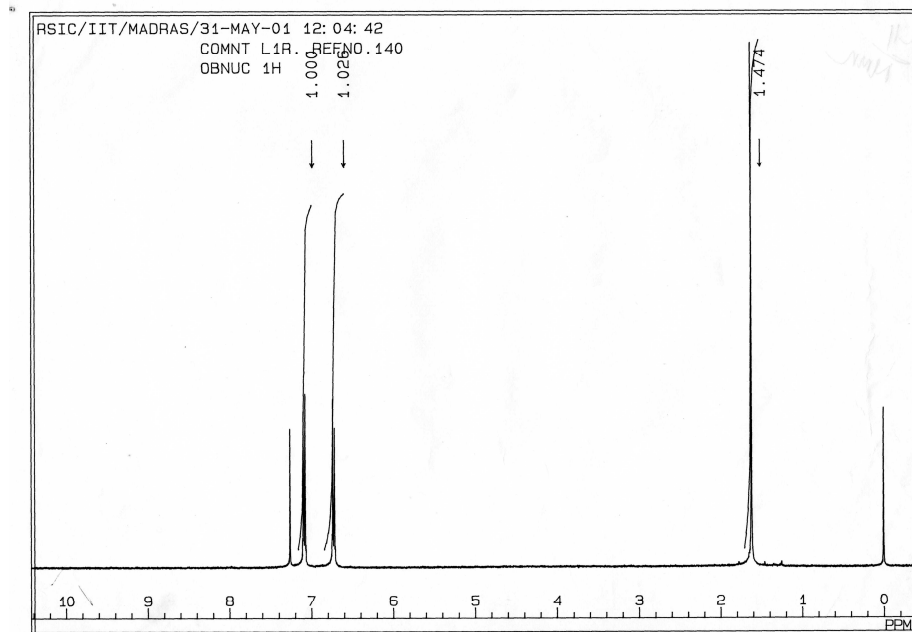


Figure 1. ^1H NMR Spectrum of LH_2 .

Powder XRD studies

The XRD (powder pattern) of the complex $[\text{Cd}_2\text{LCl}_2(\text{H}_2\text{O})_2]$ was indexed in X-ray diffractometer with Cu as anode material, K - alpha [\AA] = 1.54060 and the generator settings 30 mA, 40 kV. The prominent peaks (Figure 2) of the diffraction pattern were indexed and analysed by the computer programme LSUCRPC [34]. The lattice parameters (a, b, c, α , β , γ and V (volume) are shown in (Table 2) along with Miller indices h k l. The indexing is confirmed by comparing with observed and calculated 2θ values that are evident from the figure of merit 5.8 as suggested by de Wolff [35]. The observed and calculated 2θ values are also in good agreement. The density (d) of the complex was determined by the floatation method in a saturated solution of KBr, NaCl and benzene separately. The number of formula units per unit cell (n) is calculated from the relation:

$$n = dNV/M$$

where d = density of the compound, N = Avogadro's number, V = volume of the unit cell and M = molecular weight of the complex. The value of 'n' is found to be '1' that agrees well with the suggested orthorhombic structure of the complexes. The mean particle size of the same complex can be measured from the Debye Scherrer equation:

$$D = K\lambda/\beta \cos \theta$$

where D = particle size, K = dimensionless shape factor, λ = X-ray wavelength, β = line broadening at half the maximum intensity, θ = diffraction angle. This equation relates the size of the particle in a solid in the broadening of a peak in a diffraction pattern. The particle size of the complex $[\text{Cd}_2\text{LCl}_2(\text{H}_2\text{O})_2]$ is found to be 11.2 nm [36].

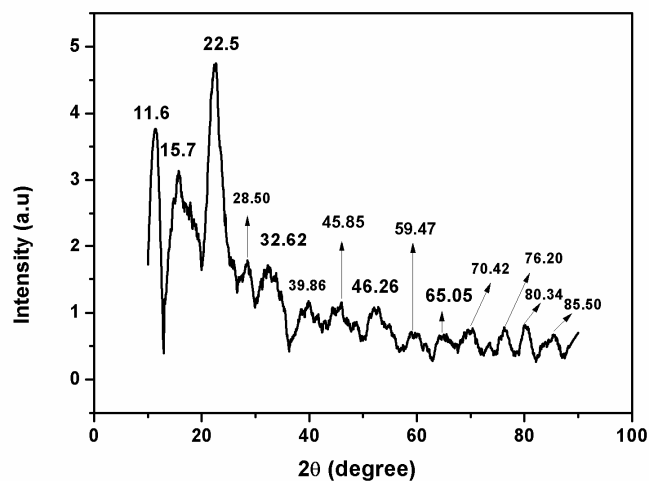


Figure 2. XRD Graph of $[\text{Cd}_2\text{LCl}_2(\text{H}_2\text{O})_2]$.

Table 2. X-ray diffraction data of the complex.

Observed 2θ	Calculated 2θ	d-spacing	h k l	Difference (2θ)
11.69	11.68	7.573	1 1 0	0.01
15.83	15.81	5.600	1 3 0	0.02
22.53	22.52	3.943	2 1 0	0.01
33.82	33.81	2.649	3 1 0	0.01
39.86	39.84	2.258	2 1 -1	0.02
44.22	44.21	2.044	2 5 -1	0.01
45.85	45.84	1.975	3 8 0	0.04
46.26	46.21	1.960	0 12 0	0.05
48.82	48.81	1.863	3 3 -1	0.01
49.12	49.11	1.852	3 3 1	0.01
59.47	59.43	1.552	2 11 1	0.04
65.05	65.04	1.433	0 14 1	0.01
70.42	70.41	1.336	0 4 2	0.01
73.57	73.54	1.287	4 11 1	0.03
76.20	76.19	1.249	2 5 2	0.01
80.34	80.33	1.194	5 10 -1	0.01
85.50	85.48	1.134	4 10 -2	0.02

$a = 8.860 \text{ \AA}$, $\alpha = 90^\circ$, volume = 1078.74 \AA^3 , Bravais lattice = P, $b = 14.349 \text{ \AA}$, $\beta = 90^\circ$, density = 1.422 g/cm^3 , figure of merit = 5.8, $c = 8.473 \text{ \AA}$, $\gamma = 90^\circ$, number of unit cell (n) = 1, crystal system = orthorhombic.

Thermogravimetric studies

The thermal decomposition behaviour of the complex $[\text{Cd}_2\text{LCl}_2(\text{H}_2\text{O})_2]$ was studied by using TG and DTA techniques in static atmosphere of nitrogen at a heating rate of $10 \text{ }^\circ\text{C/min}$ (Figure 3). The mass loss in complex compound was recorded from in ambient temperature to $1200 \text{ }^\circ\text{C}$.

The complex remains stable up to 200 °C and suffered a mass loss of 11.95% at about 200–300 °C that correspond to loss of two water molecules and 8% of the ligand supported by an endothermic peak at 300 °C. Then the compound remained stable up to 600 °C. Thereafter, the compound losses almost all its masses gradually between 600–700 °C supported by endothermic peak at 600 °C. Finally, the thermogram becomes a straight line after 700 °C.

The kinetic parameters as order of the reaction (n) and activation energy (E_a) can be calculated by Freeman-Carroll method [37]. The given equation used for this purpose is

$$-dw/dt = R_T = Z/R_H e^{-E_a/RT} W^n$$

Where R_H = rate of heating, W = weight fraction of the reacting material, E_a = activation energy and Z = frequency factor. This equation in the difference form can be written as

$$\Delta \log R_T = n \Delta \log W - E_a/2.303R\Delta(1/T)$$

When $\Delta(1/T)$ is kept constant a plot of $\Delta \log R_T$ versus $\Delta \log W$ gives a linear relationship whose slope and intercept provides the value of n and E_a , respectively. The order of decomposition reaction and the activation energy are found to be 1.22 and 4.728 J/mol, respectively. The calculated value of activation energy is found to be low attributable to auto-catalytic effect of the metal ion on the thermal decomposition of the complex [38]. The correlation factor (r) is found to be 0.99 and the thermal decomposition of the complex fits well with the experimental results. The non-volatile nature of the complex is indicated from the thermal stability of the complex.

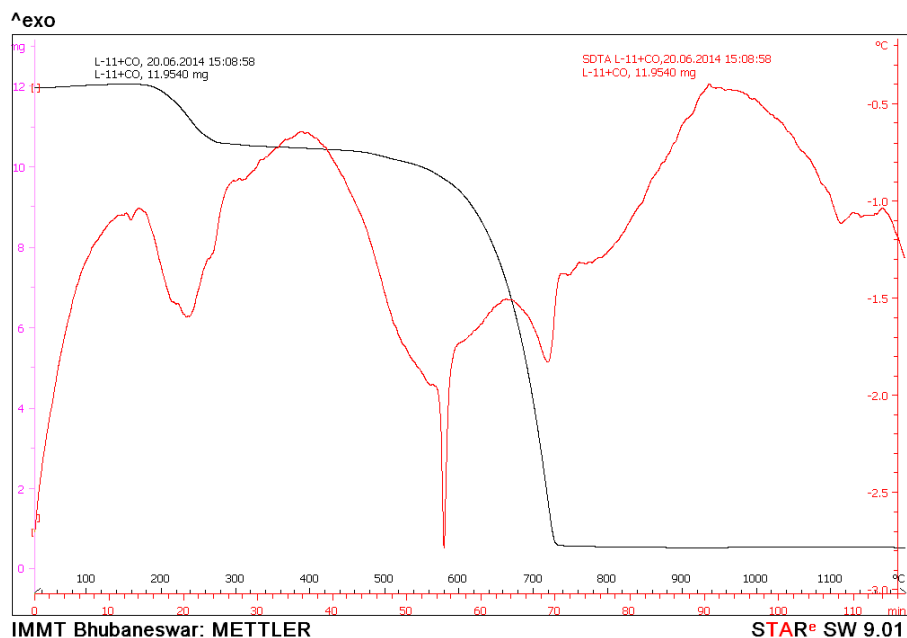


Figure 3. TGA of $[Cd_2LCl_2(H_2O)_2]$.

Theoretical calculation

Geometrical optimization

The ligand and its Cu(II) and Zn(II) complexes are optimized at B3LYP/6-31G (d, p) and B3LYP/LANL2DZ level in gas phase to get the stable geometry. Geometrical parameters of the

ligand and its Cu(II) complex and Zn(II) complex (Figure 4) are collected from the stable geometry (Table 3 and 4). It is observed that the bond lengths such as C5-O12, C5-C2, C2-N8, N8-C13, N13-C16 of the ligand have undergone a change in Cu(II) and Zn(II) complexes that indicates the coordination of the ligand donor atoms with the metal ions [39, 40]. This fact has been supported by vibrational frequencies in I.R. spectra of the complexes. The bond angles such as O11-Cu34-N12, N12-Cu34-Cl36, O38-Cu34-O41, N12-Cu34-O38 for the Cu(II) ion and the bond angles such as O11-Zn34-N12, N12-Zn34-Cl36, Cl36-Zn34-O38, O11-Zn34-O38 for the Zn(II) ions suggests a distorted-octahedral and distorted-tetrahedral geometry around the Cu(II) and Zn(II) ions respectively [39, 40].

The single point energy and dipole moment of the ligand and its Cu(II) and Zn(II) complexes were calculated using DFT/B3LYP 6-31G (d, p) and DFT/B3LYP LANL2DZ basic sets. The single point energy of both the complexes were found to be less than the energy of the ligand which confirms more stability of complexes than the free ligand. The higher dipole moment of the complexes than the free ligand indicates stronger dipole-dipole interaction after complexation. Also it is observed that the Zn(II) complex possess higher dipole moment values in both the methods than the Cu(II) complex that indicates that Zn(II) complex is found to be less covalent than the Cu(II) complex.

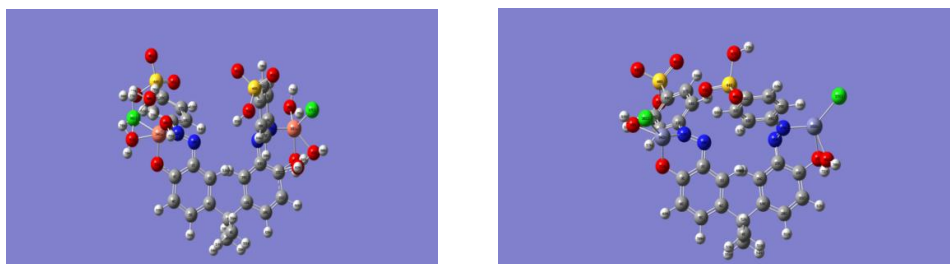


Figure 4. Optimised geometry of the Zn(II) complex and of the Cu(II) complex, respectively.

Table 3. Selected bond length (Å) and bond angle (degree) of the ligand (LH₂).

B3LYP / 6.31G (d, p)	
Bond length (Å)	Bond Angle (°)
C5-O12 (1.354)	O12-C5-C2 (124.331)
C5-C2 (1.337)	C5-C2-N8 (119.939)
C2-N8 (1.260)	C2-N8-N13 (107.543)
N8-C13 (1.247)	N8-N13-C16 (106.757)
N13-C16 (1.258)	

Chemical reactivity study

The E_{HOMO} and E_{LUMO} energy of the ligand and its Cu(II) and Zn(II) complexes are calculated to evaluate the global reactivity descriptors as chemical hardness, electrochemical potential, electrophilicity and chemical hardness. Calculation of molecular orbital coefficients indicates that the possible coordination sites of the ligand are -N=N- (azo) and C-O (phenolic) group [41, 42] that binds the metal ion. Since the E_{HOMO} and E_{LUMO} values are found negative that indicate the ligand and its complexes are stable [41, 42]. The decrease of E_{HOMO} values of the complex compounds with the value of the ligand that confirms the weakening of metal-ligand sites. The HOMO level for the ligand is localized on the N₈, N₁₃, O₁₂, N₄₀, N₅₂ and O₅₁ (Figure 5) indicates that these are the preferred bonding sites for the nucleophilic attack. The energy gap between

E_{HOMO} and E_{LUMO} is an important parameter to determine the chemical reactivity and chemical stability of the molecule [43]. The energy gap [$E_{\text{HOMO}} - E_{\text{LUMO}}$] of the ligand is found to be less than the energy gap of the complexes that indicates greater reactivity of the ligand than the complexes and hence more stability of the complexes (Figures 6 and 7).

Table 4. Selected bond length (Å) and bond angle (degree) of $[\text{Cu}_2\text{LCl}_2(\text{H}_2\text{O})_6]$ and $[\text{Zn}_2\text{LCl}_2(\text{H}_2\text{O})_2]$.

$[\text{Cu}_2\text{LCl}_2(\text{H}_2\text{O})_6]$ B3LYP/LANL2DZ		$[\text{Zn}_2\text{LCl}_2(\text{H}_2\text{O})_2]$ B3LYP/LANL2DZ	
Bond length (Å)	Bond Angle (°)	Bond length (Å)	Bond Angle (°)
N10-N12 (1.159)	Cu34-N12-N10 (134.530)	N10-N12 (1.247)	Zn34-N12-N10 (127.714)
C2-N10 (1.248)	N12-N10-C2 (111.630)	C2-N10 (1.259)	N12-N10-C2 (107.503)
C2-C3 (1.343)	C2-C3-O11 (123.275)	C2-C3 (1.336)	C2-C3-O11 (124.294)
C3-O11 (1.344)	C3-O11-Cu34 (113.755)	C3-O11 (1.354)	C3-O11-Cu34 (109.490)
C13-N12 (1.236)	O11-Cu34-N12 (79.818)	C13-N12 (1.260)	O11-Zn34-N12 (69.817)
Cu34-O11 (1.781)	N12-Cu34-Cl36 (113.236)	Zn34-O11 (1.890)	N12-Zn34-Cl36 (145.087)
Cu34-N12 (1.557)	Cl36-Cu34-O38 (113.773)	Zn34-N12 (1.753)	Cl36-Zn34-O38 (68.176)
Cu34-Cl36 (2.011)	O38-Cu34-O41 (113.988)	Zn34-Cl36 (2.240)	
Cu34-O38 (1.805)	N12-Cu34-O38 (111.725)	Zn34-O38 (1.890)	
Cu34-O41 (1.794)	O11-Cu34-O38 (134.118)		

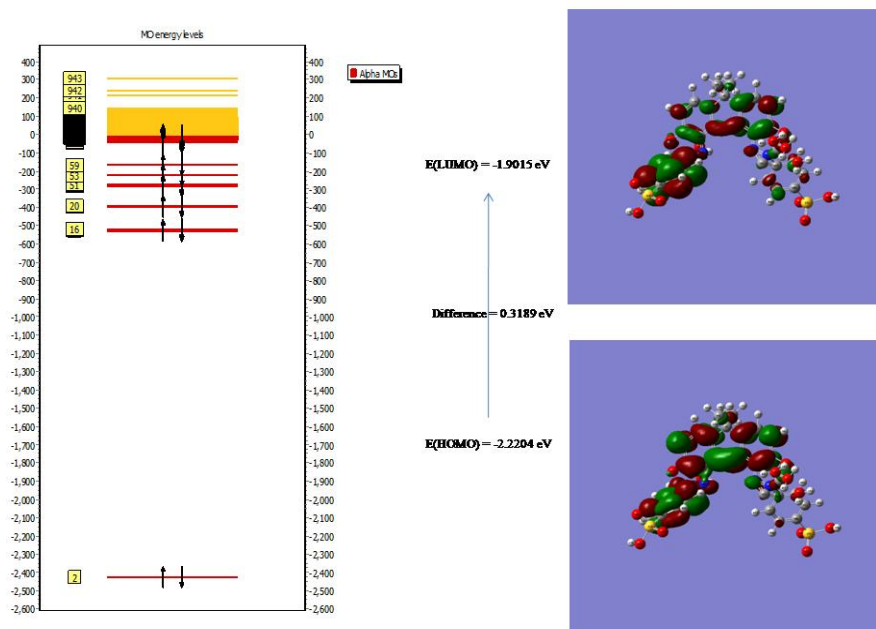


Figure 5. Molecular orbital energy level diagram with HOMO and LUMO orbital of LH₂.

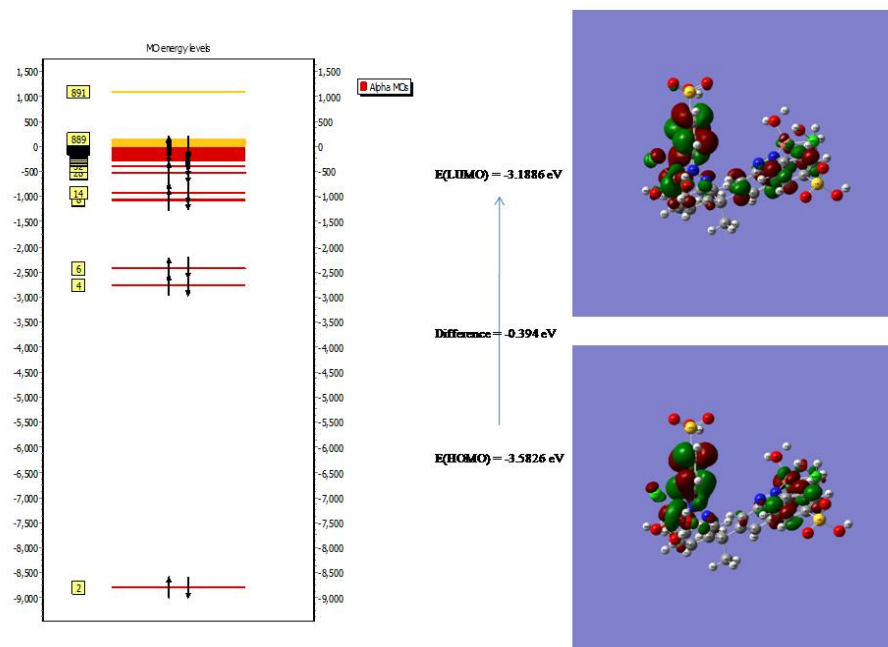


Figure 6. Molecular orbital energy level diagram with HOMO and LUMO orbital of Cu(II) complex.

The DFT/B3LYP method indicates the chemical reactivity and the selection of active sites of the molecular system. The energy of FMOs and the energy band gap explain the charge transfer interaction within the molecule. The chemical reactivity values as electronegativity (χ), chemical potential (μ), global hardness (η), global softness (S) and global electrophilicity index (ω) [44, 45] are listed in (Table 5).

$$\chi = (E_{\text{LUMO}} + E_{\text{HOMO}})/2$$

$$\mu = -\chi = (E_{\text{LUMO}} + E_{\text{HOMO}})/2$$

$$\eta = (E_{\text{LUMO}} - E_{\text{HOMO}})/2$$

$$S = 1/2\eta$$

$$\omega = \mu^2/2\eta$$

$$\sigma = 1/\eta$$

Table 5. Calculated quantum chemical parameters for ligand and its metal complexes.

Compound	HOMO in eV	LUMO in eV	ΔE in eV	χ Pauling	η in eV	σ	μ in eV	S	ω eV
LH ₂	-2.2204	-1.9015	0.3189	-2.0609	0.1594	6.2735	2.0609	3.1367	13.3227
[Cu ₂ LCl ₂ (H ₂ O) ₆]	-3.5826	-3.1886	0.394	-3.3856	0.197	5.0761	3.3856	2.538	29.0918
[Zn ₂ LCl ₂ (H ₂ O) ₂]	-4.0784	-3.5307	0.5477	-3.8045	0.2738	3.6523	3.8045	1.8261	26.432

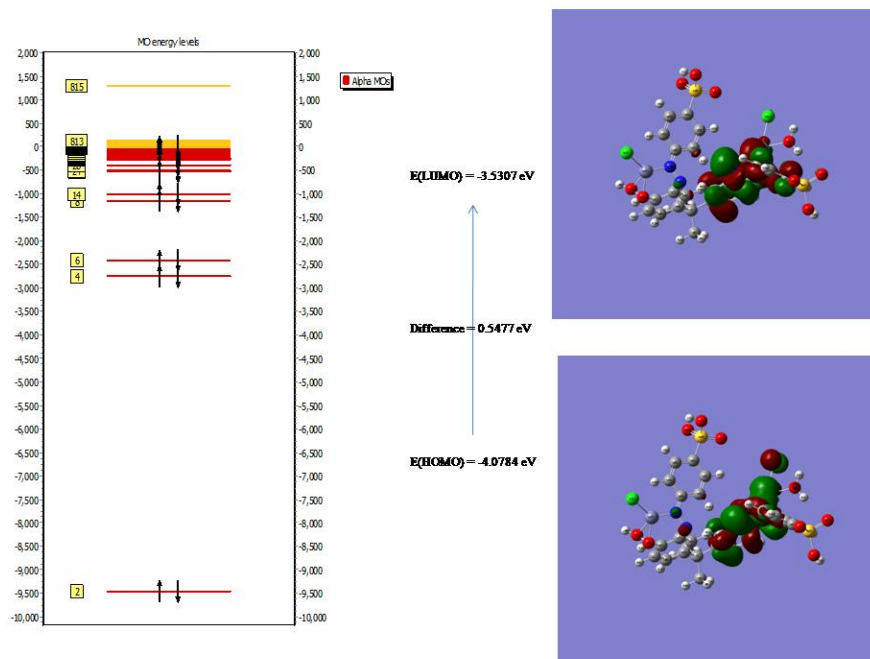


Figure 7. Molecular orbital energy level diagram with HOMO and LUMO orbital of Zn(II) complex.

Table 6. Energetic properties of the ligand (LH₂) and its [Cu₂LCI₂(H₂O)₆] and [Zn₂LCI₂(H₂O)₂] complexes calculated by DFT/B3LYP 6.31G (d, P) and DFT/B3LYP LANL2DZ basic sets.

Compound	Single point energy in kcal/mol		Dipole moment (D)	
	DFT/B3LYP 6.31G (d, P)	DFT/B3LYP LANL2DZ	DFT/B3LYP 6.31G (d, P)	DFT/B3LYP LANL2DZ
LH ₂	-2.0469×10 ⁶	-	5.936	-
[Cu ₂ LCI ₂ (H ₂ O) ₆]	-4.5886×10 ⁶	-1.7297×10 ⁶	22.014	18.659
[Zn ₂ LCI ₂ (H ₂ O) ₂]	-4.5734×10 ⁶	-1.3766×10 ⁶	23.508	25.429

The E_{HOMO} and E_{LUMO} plots and the MO diagram (Figure 5, Figure 6 and Figure 7) of the ligand, Cu(II) and Zn(II) complexes show the exact energy gap between the orbitals. The chemical softness (S) of the ligand is higher than the complexes therefore it reacts effectively with the metal ion forming the stable complexes which is confirmed from their chemical potential (μ) value. The electrophilicity (ω) is a positive quantity that measures the tendency of a system to accept electron from the environment. The Zn(II) complex is found to be more stable than the Cu(II) complex as it possess less electrophilicity value than Cu(II) complex (Table 6).

CONCLUSION

The tetradentate ligand (4,4'-(1E,1'E)-(5,5'-(propane-2,2-diyl)bis(2-hydroxy-5,1-phenylene)-bis(diazene-2,1-diyl)dibenzene)sulfonic acid) and its six dimeric stable complexes were

synthesized and their structures have been confirmed by elemental analysis, IR, electronic, ^1H NMR and ESR spectra. The stability of the complexes was confirmed from the thermal study. The kinetic parameters such as activation energy (E_a) and order of reaction (n) were determined from the thermal decomposition data. The XRD study shows that the Cd(II) complex is orthorhombic in nature. The theoretical study using DFT/B3LYP supports experimental evidences of the bonding sites of the ligand, geometry and the stability of the complexes. The quantum chemical parameters reported here will be helpful to the future investigators working in the field of drug designing.

ACKNOWLEDGEMENTS

The authors are thankful to The Head, SAIF, and I.I.T. Madras, India for providing spectral analysis and thermogravimetric analysis and MMIT, Bhubaneswar, India for kind help of XRD analysis.

REFERENCES

1. Al-Harbi, L.M.; El-Mossalamy, E.H.; Ahmed, I.S.; Obaid, A.Y. *Am. J. Anal. Chem.* **2013**, *4*, 427.
2. Goodman, L.S.; Gilman, A. *The Pharmacological Basis of Therapeutics*, 5th ed., MacMillan: New York; **1970**; p 472.
3. Isa, R.M.; Dessouki, H.A.; Ghoneium, A.K.; Moustafa, M.M. *J. Indian Chem. Soc.* **1984**, *61*, 286.
4. "Bisphenol A Information Sheet". Bisphenol A Global Industry Group; October **2002**. Available at: <http://www.bisphenol-a.org/pdf/DiscoveryandUseOctober2002.pdf>; accessed on December 7, 2010.
5. Wendell, B.; Halbrook, Jr.; Mary, Ann Wehr *Thermal paper with security features*, Publication patent no US 6562755, , Application number US 09/699, 486, Publication date 13 May **2003**, Filing date 31 Oct **2000**, Priority date 31 Oct **2000**.
6. Raloff, J. *Concerned about BPA: Check your receipts*, Science News (Magazine of the Society for Science & the Public). Available at: <https://www.sciencenews.org/blog/science-public/concerned-about-bpa-check-your-receipts>; accessed on August 3, **2010**.
7. Sulphanilic acid *A Dictionary of Chemistry*, Oxford University Press: Oxford Reference Online; **2000**; pp. 508.
8. Mahapatra, B.B.; Mishra, R.R.; Sarangi A.K. *J. Saudi Chem. Soc.* **2013**, <http://dx.doi.org/10.1016/j.jscs.2013.07.002>; Mahapatra, B.B.; Mishra, R.R.; Sarangi A.K. *J. Chem.* **2013**, Article ID 653540, 2013, 1; <http://dx.doi.org/10.1155/2013/653540>, Mahapatra, B.B.; Chaulia, S.N.; Sarangi, A.K.; Dehury, S.N.; Panda, J.R. *J. Mol. Struct.* **2015**, <http://dx.doi.org/10.1016/j.molstruc.2015.01.030>.
9. *GaussView 5.0*, Gaussian Inc.: Wallingford, CT, USA; **2009**.
10. Becke, A.D. *J. Chem. Phys.* **1993**, *98*, 5648.
11. Lee, C.T.; Yang, W.T.; Parr, R.G. *Phys. Rev. B* **1988**, *37*, 785.
12. Becke, A.D. *Phys. Rev. A* **1988**, *38*, 3098.
13. Hay, P.J.; Wadt, W.R. *J. Chem. Phys.* **1985**, *82*, 270.
14. Hay, P.J.; Wadt, W.R. *J. Chem. Phys.* **1985**, *82*, 284.
15. Hay, P.J.; Wadt, W.R. *J. Chem. Phys.* **1985**, *82*, 299.
16. Frisch, M.J.; Trucks, G.W.; Schlegel, H.B.; Scuseria, G.E.; Robb, M.A.; Cheeseman, J.R.; Montgomery Jr, J.A.; Vreven, T.; Kudin, K.N.; Burant, J.C.; Millam, J.M.; Iyengar, S.S.; Tomasi, J.; Barone, V.; Mennucci, B.; Cossi, M.; Scalmani, G.; Rega, N.; Petersson, G.A.; Nakatsuji, H.; Hada, M.; Ehara, M.; Toyota, K.; Fukuda, R.; Hasegawa, J.; Ishida, M.; Nakajima, T.; Honda, Y.; Kitao, O.; Nakai, H.; Klene, M.; Knox, X. Li. JE.; Hratchian, H.P.; Cross, J.B.; Adamo, C.; Jaramillo, J.; Gomperts, R.; Stratmann, R.E.; Yazyev, O.; Austin,

- A.J.; Cammi, R.; Pomelli, C.; Ochterski, J.W.; Ayala, P.Y.; Morokuma, K.; Voth, G.A.; Salvador, P.; Dannenberg, J.J.; Zakrzewski, V.G.; Dapprich, S.; Daniels, A.D.; Strain, M.C.; Farkas, O.; Malick, D.K.; Rabuck, A.D.; Raghavachari, K.; Foresman, J.B.; Ortiz, J.V.; Cui, Q.; Baboul, A.G.; Clifford, S.; Cioslowski, J.; Stefanov, B.B.; Liu, G.; Liashenko, A.; Piskorz, P.; Komaromi, I.; Martin, R.L.; Fox, D.J.; Keith, T.; Al-Laham, M.A.; Peng, C.Y.; Nanayakkara, A.; Challacombe, M.; Gill, P.M.W.; Johnson, B.; Chen, W.; Wong, M.W.; Gonzalez, C.; Pople, J.A.; GAUSSIAN 03, Revision E.01, Gaussian Inc.: Pittsburgh, PA, **2004**.
17. Mishra, L.K.; Keshari, B.N. *Indian J. Chem. A* **1981**, 28, 883.
18. King, R.B.; Bisnette, M.B. *Inorg. Chem.* **1966**, 5, 300.
19. Nakamoto, K. *Infrared and Raman Spectra of Inorganic and Coordination Compounds*, John Wiley and Sons: New York; **1978**; p 239.
20. Ferraro, J.R. *Low Frequency Vibration of Inorganic and Co-Ordination Compound*, Plenum Press: New York; **1971**; p 321.
21. König, E. *Structure & Bonding*, Vol. 9, Springer: Germany; **1970**; p 175.
22. Atkins, P.J.; Shriver, D.F. *Inorganic Chemistry*, 3rd ed. W.H. Freeman and Company: New York; **1999**.
23. Lever, A.B.P. *Inorganic Electronic Spectroscopy*, Elsevier: Amsterdam; **1984**; p 554.
24. Magee, R.; Gordan, L. *Talanta* **1963**, 10, 967.
25. Yamada, S. *Coord. Chem. Rev.* **1966**, 1, 415.
26. Procter, I.M.; Hathaway, B.J.; Nicholls, P. *J. Chem. Soc.* **1968**, 1678.
27. a) Vinuelas-Zahinos, E.; Maldonado-Rogado, M.A.; Luna-Giles, F.; Barros-Garcia, F.J. *Polyhedron* **2008**, 27, 879; b) Avaji, P.G.; Patil, S.A.; Badami, P.S. *Transit. Met. Chem.* **2008**, 33, 275.
28. Tavman1, A.; Gürbüz, D.; Çınarlı, A.; Tan, S.B. *Bull. Chem. Soc. Ethiop.* **2015**, 29, 63.
29. Williams, D.H.; Fleming, I. *Spectroscopic Methods in Organic Chemistry*, Tata McGraw Hill: 4th ed., New Delhi; **1994**; p 1.
30. Jacob, W.; Mukherjee, R. *Inorg. Chim. Acta* **2006**, 359, 4565.
31. Dash, U.N. *Analytical Chemistry: Theory and Practice*. 1st ed., Sultan Chand and Company Ltd.: New Delhi; **1995**; pp. 143-173.
32. Kneubuhl, F.K. *J. Chem. Phys.* **1960**, 33, 1074.
33. Dutta, R.L.; Syamal, A. *Elements of Magnetochemistry*, Sultan Chand and Company Ltd.: New Delhi; **1982**; p 96.
34. Visser, J.W. *J. Appl. Crystal.* **1969**, 2, 89.
35. de Woulff, P.M. *J. Appl. Crystal.* **1968**, 1, 108.
36. Patterson, A. *Phys. Rev.* **1939**, 56, 978.
37. Freeman, E.S.; Carroll, B. *J. Phys. Chem.* **1958**, 62, 394.
38. Iimura, A.; Inoue, Y.; Yasumori, I. *Bull. Chem. Soc. Jpn.* **1983**, 56, 2203.
39. Yousef, T.A.; Rakha, T.H.; El Ayaan, U.; Abu El Reash, G.M. *J. Mol. Struct.* **2012**, 1007, 146.
40. Yousef, T.A.; Abu El-Reash, G.M.; Rakha, T.H.; El-Ayaan, U. *Spectrochim. Acta* **2011**, 83, 271.
41. Yousef, T.A.; Abu El-Reash, G.M.; El Morshedy, R.M. *Polyhedron* **2012**, 45, 71.
42. Yousef, T.A.; Abu El-Reash, G.M.; El Morshedy, R.M. *J. Mol. Struct.* **2013**, 1045, 145.
43. Govindarajan, M.; Periandy, S.; Carthigayen, K. *Spectrochim. Acta Part A Mol. Biomol. Spectrosc.* **2012**, 97, 411.
44. Pearson, R.G. *J. Org. Chem.* **1989**, 54, 1423.
45. Padmanabhan, J.; Parthasarathi, R.; Subramanian, V.; Chattaraj, P. *J. Phys. Chem.* **2007**, A 111, 1358.